

Energy spectrum, magnetic characteristics, and spin dynamics of lightly doped 2:1:4 oxides

V. Barzykin and L. P. Gor'kov

*Department of Physics and Materials Research Laboratory, University of Illinois at Urbana-Champaign,
1110 West Green Street, Urbana, Illinois 61801*

*and L. D. Landau Institute for Theoretical Physics, Academy of Sciences of Russia, 117 334 Moscow,
Kosygina Street 2, Russia*

(Received 3 February 1992)

Analyses of ^{63}Cu and ^{17}O relaxation rates, as measured by NMR probes, prove unambiguously that in conducting $\text{YBa}_2\text{Cu}_3\text{O}_{7-x}$ and $\text{La}_{1.85}\text{Sr}_{0.15}\text{CuO}_4$ the Cu^{2+} ions still possess a magnetic moment that exhibits antiferromagnetic fluctuations. We discuss the corresponding characteristics in the low-doped regime from the side of the Mott-insulator state, where the local moments are expected to be even more pronounced. Both neutrons and NMR probes measure the imaginary part of the generalized magnetic susceptibility. We have investigated the contribution to the dissipation due to added holes. Then, depending on the hole spectrum chosen, both bulk and staggered static susceptibilities in the high-temperature paramagnetic phase are strongly concentration dependent. The corresponding exchange-integral components in the absence of holes can be strongly enhanced, but their signs do not always lead to an instability. At the same time, the imaginary part of the generalized susceptibility, as determined by the hole spectrum, behaves independently and can provide strong peaks at some wave vectors even if the static part has no singular behavior there. We identify the single model energy spectrum, which is compatible with the properties of 2:1:4 materials, and discuss the "metallization" of $\text{La}_{2-x}\text{Sr}_x\text{CuO}_4$ with the increase in strontium concentration. While the transport properties can be understood in terms of carriers present in the conducting bands, the static magnetic susceptibility behavior reveals the overwhelming role of spin-spin correlations. Shortcomings of the model are also discussed.

I. INTRODUCTION

In what follows we address some properties of 2:1:4-based oxides ($\text{La}_{2-x}\text{Sr}_x\text{CuO}_4$, $\text{La}_2\text{CuO}_{4+\delta}$, etc.) in the regime of low dopant concentrations. The parent compound La_2CuO_4 provides an important example of a Mott-type insulating state possessing a Néel antiferromagnetic (AF) ground state for the localized Cu^{2+} states.¹ In Fermi-liquid frameworks the compound would be a half-filled-band metal.

The phase transition between the insulating and metallic ground states has been observed in the solutions of oxygen, $\text{La}_2\text{CuO}_{4+\delta}$, at rather low concentrations of oxygen, δ . The schematic phase diagram (from Refs. 2 and 3) is shown in Fig. 1. Recently, it has been reported⁴ that the orthorhombic phases *O* I and *O* II have identical symmetry. If it were so, then this would probably be the ultimate proof that the temperature, T_k , is the critical point of a first-order Mott-type phase transition. The reasons why the two phases (metal and insulator) are so close in energy to each other [$T_k \approx 280\text{--}300$ K (Refs. 5 and 6)] still remain unclear. The actual visualization (i.e., the phase separation) of this transition in $\text{La}_2\text{CuO}_{4+\delta}$ is, without doubt, the direct consequence of a high enough oxygen mobility in the system. It is not the case for strontium ions in $\text{La}_{2-x}\text{Sr}_x\text{CuO}_4$ systems. Nevertheless, systematic "metallization" with the increase of strontium concentration has been repeatedly reported⁷ and the metallic phase with the so-called "optimal" concentration,

$\text{La}_{1.85}\text{Sr}_{0.15}\text{CuO}_4$, provides one of the most studied examples of recently discovered superconductors. One would, however, conclude from the above considerations that the metallic state evolving with a decrease of strontium concentration is not to merge smoothly with a phase developing if one departs from the stoichiometric composition. Therefore one of the goals of this paper is to discuss a number of physical characteristics of the low-doped system using a simple but reasonable model for the energy spectrum in the insulating phase.

Among numerous experimental facts available now for these oxides in the normal state, we would like to single out the NMR studies of $\text{YBa}_2\text{Cu}_3\text{O}_{7-\delta}$ and $\text{La}_{1.85}\text{Sr}_{0.15}\text{CuO}_4$ and the theoretical analyses done in this connection in Ref. 9 (see Ref. 10 and the review in Ref. 8 for experimental references). As a local probe method, the NMR [nuclear quadrupole resonance (NQR)] technique provides information on the spin subsystem and its dynamics. On the other hand, the Millis-Monien-Pines (MMP) analyses⁹ based solely on the Mila-Rice Hamiltonian,¹¹ which is expressed in terms of localized spins only, unambiguously testifies that the local moments are still present even in the metallic conducting regime. This conclusion stems from the significant difference in magnitude and temperature behavior for the relaxation rates $^{63}\text{T}_1^{-1}$ and $^{17}\text{T}_1^{-1}$, which were understood in terms of enhanced relaxation on the Cu sites ascribed to antiferromagnetic (AF) fluctuations. However, the actual source of dissipation [i.e., $\chi'' = \text{Im}\{\chi(\mathbf{q}, \omega)\}$] is more likely due to the contribution of conducting electrons than due to

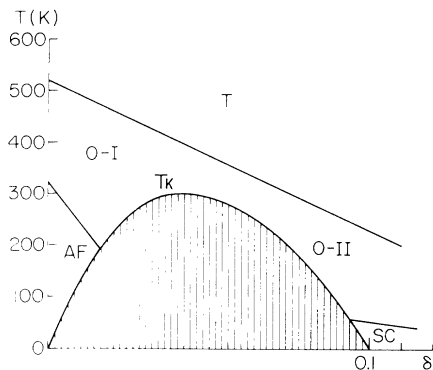


FIG. 1. Phase diagram of $\text{La}_2\text{CuO}_{4+\delta}$. The hatched region is the region of an O I–O II phase stratification.

solely spin-spin relaxation, as it follows from the drastic change in the behavior of all relaxation rates below the temperature of superconducting transition. These features are summarized in MMP theory as a state of “almost localized holes,” meaning that spins and conducting holes somehow create a one-component system. With this picture in mind, it seems that these peculiarities are to be somehow even more pronounced in the range of small hole concentrations. To the best of our knowledge, nobody has so far traced this tendency experimentally with the systematic decrease of x in $\text{La}_{2-x}\text{Sr}_x\text{CuO}_4$ from the metallic side (see Ref. 12, however). In any case it is clear that with the further decrease of concentration, one would meet a phase-transition problem, as described above.

Below we consider the magnetic susceptibility $\chi(T, \mathbf{q}, \omega)$, i.e., its momentum, frequency, and temperature dependence from the side of low-doped insulating phase. In accordance with the diagram in Fig. 1, it may happen that the regime under investigation is available only at high enough temperatures. To separate the main qualitative features, we assume first a simple band model¹³ in the hope that progress in sample preparation will make it possible to distinguish among various options of this model. It also seems that our results could be applicable to the 1:2:3 materials if it were possible to establish a reliable “mapping”—a sort of equivalence between the Mott state of La_2CuO_4 and the corresponding oxygen concentration for $\text{YBa}_2\text{CuO}_{7-x}$ ($\text{O}_{6.5}$?).

The essential difference between $\text{La}_2\text{CuO}_{4+\delta}$ and $\text{La}_{2-x}\text{Sr}_x\text{CuO}_4$ is that in the former case the phase transition realizes as a spatial phase separation, while in the case of $\text{La}_{2-x}\text{Sr}_x\text{CuO}_4$ the strontium ions are not mobile, at least at room temperature (compare, however, the discussion in Refs. 6 and 7). We address therefore the issue whether the “metallization” of $\text{La}_{2-x}\text{Sr}_x\text{CuO}_4$ has something in common with the first-order phase transition for $\text{La}_2\text{CuO}_{4+\delta}$ in Sec. VII.

In Sec. II we remind the phenomenological model^{13–15} of the conduction-hole energy spectrum in the insulating phase and give arguments that it correctly describes the main transport properties. The model is a sort of “rigid-band” picture and is accepted as a start for further specu-

lations. Nevertheless, this approach accounts for the fact that the energy spectrum in the recently described oxides is probably closer to “charge-transfer-” (CT-) insulator scheme, as introduced in Ref. 16, than to the Hubbard-model description. In Secs. III–V we enumerate various possibilities for the choice of energy spectrum and describe the main features of the resulting spin-spin exchange interaction and its concentration dependence. It is shown that the conduction-hole contribution to the imaginary part of the generalized magnetic susceptibility behaves independently of the peculiarities, say, of the static part, reflecting specific features of the forming Fermi surfaces. As mentioned above, in the metallic regime the conduction-hole contribution dominates at low enough temperatures, and we briefly discuss in Sec. VI some anomalies for the $\chi''(\mathbf{q}, \omega)$ behavior which would reflect the shape of the Fermi surface, if it exists. Section VII is devoted to the issue of “merging” the Mott state possessing localized moments with the “metallic” regime at the change of dopant concentration. We also conclude that the only energy spectrum which seems to be compatible with the overall properties of $\text{La}_{2-x}\text{Sr}_x\text{CuO}_4$ is that of Sec. III. Both Secs. VII and VIII contain a brief summary of the results obtained and the discussion of shortcomings of the “rigid-band” model, as regards the concentration dependence and the growth of AF fluctuations in the temperature region of experimental interest.

II. MODEL

As mentioned above, we intend to use the model suggested in Ref. 13 (see also Ref. 17). In such a model the localized moments would occupy slightly hybridized single levels with almost empty conduction bands. In next sections, to enrich the number of options of the model, we introduce at least two conduction bands. In a mathematical sense the model can always be expressed in terms of an Anderson-type Hamiltonian:

$$\begin{aligned}
 H = & \sum_{n,\sigma} \varepsilon_0 d_{n\sigma}^\dagger d_{n\sigma} + \sum_{\mathbf{p},\sigma,i} \varepsilon_{\mathbf{p}i} a_{\mathbf{p}\sigma i}^\dagger a_{\mathbf{p}\sigma i} \\
 & + \frac{1}{N^{1/2}} \sum_{\mathbf{p},n,\sigma,i} V_i \{ a_{n\sigma i}^\dagger d_{n\sigma} e^{-i\mathbf{p}\cdot\mathbf{R}_n} + \text{H.c.} \} \\
 & + \sum_n U d_{n\uparrow}^\dagger d_{n\downarrow}^\dagger d_{n\downarrow} d_{n\uparrow}. \quad (1)
 \end{aligned}$$

(In what follows we choose $U = \infty$.)

Let us first briefly give arguments why this model seems to be reasonable to start with. Remember that one departs from the Mott-insulator state. The localization of the carriers in this system is the consequence of the strong interaction of the d orbitals on the Cu^{2+} ion. The wave function for the localized state is, of course, different from that of the hole in the d^9 configuration for an isolated copper ion. Various effects such as the hybridization, the interaction between the copper and oxygen orbitals, and shifts of the ion positions are not small, as is shown in numerous attempts to calculate the band structure. However, the localization is a qualitative effect. The conductivity is absent without dopants. If one neglects the Coulomb interaction with the dopants,

the carriers will fill the empty band with the spectrum formed primarily by the strong Coulomb correlations. The exchange interactions are therefore expected to be a weaker effect and the band energy spectrum (empty states) for the hole excitations, ε_{k_i} , can be calculated. This would be nothing but the assumption that the holes added into the so-called “upper Hubbard band” behave after renormalization as independent carriers, except for the fact that in real oxides the oxygen orbitals are much closer in energy and this provides a further support for this picture. It is worth mentioning that the concentration dependence of the Hall coefficient $R_H(x)$ in $\text{La}_{2-x}\text{Sr}_x\text{CuO}_4$, which at small x behaves as $R_H(x) \propto 1/x$ (see the review in Ref. 18) unambiguously justifies this assumption experimentally.

The introduction of small hybridization parameters V_i would then provide a regular scheme to introduce both the V_{sd} term of the order of

$$V_{sd} \sim \frac{V^2}{\Delta} (\boldsymbol{\sigma} \cdot \mathbf{S}_i) \quad (2)$$

and the exchange Heisenberg interaction between local spins,

$$\begin{aligned} H_{\text{exch}} &= \sum_{n \neq m} J(\mathbf{r}_n - \mathbf{r}_m) \mathbf{S}_n \cdot \mathbf{S}_m \\ &= \sum_{\mathbf{q}} J(\mathbf{q}) \mathbf{S}(\mathbf{q}) \cdot \mathbf{S}(-\mathbf{q}) . \end{aligned} \quad (3)$$

Here we have

$$\begin{aligned} &J(\mathbf{r}_n - \mathbf{r}_m) \\ &= -\frac{a^4}{8\pi^4} \int d\mathbf{p} d\mathbf{q} \sum_{i,j} V_i^2 V_j^2 \frac{\{1 - n(\varepsilon_{\mathbf{p}_i} - \mu)\} e^{i\mathbf{q} \cdot (\mathbf{r}_n - \mathbf{r}_m)}}{(\varepsilon_{\mathbf{p}_i} - \varepsilon_{\mathbf{p}+\mathbf{q}})(\varepsilon_{\mathbf{p}_i} - \varepsilon_0)^2} . \end{aligned} \quad (4)$$

[The derivation of Eqs. (2) and (4) has been described in detail in Ref. 14.] Among some theoretical advantages of this model, there is a possibility to vary the difference in positions of the localized level ε_0 and the bottom (the top) of the conduction band, $|\varepsilon_0 - \varepsilon_k|_{\text{min}} = \Delta$. Assuming that the conduction bands are wide enough (with the bandwidths $D \gg \Delta$), some of the interactions between spins would acquire in this model a long-range character with an effective radius $R_0 \sim a\sqrt{D}/\Delta$. In addition to that, we shall see that the exchange integral $J(\mathbf{q})$ can be made strongly peaked both at small $\mathbf{q}=0$ and for the AF vectors. The long-range character of the spin-spin interaction is, in general, not changed if holes are added since at low concentrations of carriers the Ruderman-Kittel-Kasuya-Yosida (RKKY) interaction, in its turn, also possesses long-range behavior. All those long-range interactions, hence, provide a scheme with small parameters, which therefore justifies the use of mean-field-type expressions in most of the cases and allows us to have results in the controllable approximation as opposed to the common mean-field scheme for Néel-type transitions in the presence of interactions between nearest neighbors only. In practice, of course, the actual interactions do not have a large radius. What is, however, clear is that

those interactions are also not restricted by nearest neighbors only, and with the above scheme in mind, one may, therefore, single out new qualitative features.

Introduction of a “single hole” by substitution of one Sr^{2+} for La^{3+} leads, of course, to a local distortion of the lattice. One usually argues that the Sr ion sits “far” from the CuO_2 -plane. Nevertheless, the hole is somehow to be localized not too far apart from the Sr^{2+} ion as a result of the Coulomb attraction. The decisive point, of course, is whether there is a range of concentration, x or δ , such that the hole orbits, say, on different Sr^{2+} ions essentially overlap in the “conducting” CuO_2 -plane.¹⁹ In what follows we, of course, assume that this picture of strong overlap is able to describe doping as the gradual “filling up” of the conduction bands (up to some level $\mu \propto x$). It seems that the extraordinary sensitivity of the Néel temperature to the dopant concentration to an extent favors this picture of comparatively large hole orbits and a large enough radius of interactions, as well.¹⁴

It has already been noted in Refs. 14 and 15 that arbitrary small concentrations of “dopants” can drastically change values of the exchange integral at small \mathbf{q} in Eq. (3). This is due to the fact that for almost two-dimensional (2D) systems the band density of states does not depend on concentration (for the parabolic band). We shall see that this feature remains present in our generalized model with the only exemption—Sec. III. In the next sections we consider various options for positions of conduction bands to investigate the exchange-integral components and their dependence on the hole concentrations in different situations. We address the following: (1) the temperature and concentration dependence of the static susceptibility (above the Néel temperature T_N), (2) the same problem for the “staggered” susceptibility $\chi(\mathbf{Q}_0)$ at $\mathbf{Q}_0 = (\pi, \pi)$, and (3) the temperature and concentration dependence of the imaginary part of $\chi(\mathbf{q}, \omega)$. Under the assumptions that the only source of spin dissipation is due to the charge carriers, we shall see, first, that the positions of peaks in the momentum space could be different for the static part and the imaginary contributions into the generalized magnetic susceptibility as measured, in principle, by neutrons or NMR methods. This last remark, in a sense, goes beyond the specific model choice used in the main part of our calculations and may have a relation to the recent observations of an incommensurability of magnetic fluctuations in $\text{La}_{2-x}\text{Sr}_x\text{CuO}_4$ by neutrons.²⁰ Let us stress again that the “rigid-band” model is taken below as a starting point only and could account for a regime above the onset of cooperative phenomena. We shall see later that, with concentration increase and temperature decrease, corrections to this picture are needed, especially if the 2D AF fluctuation regime rapidly develops in the system.

III. ONE EMPTY AND ONE “FILLED-UP” BAND

So far, in Refs. 13–15, only one band centered at $\mathbf{k}=0$ has been considered. The assumption $\Delta \ll D$ has resulted in strongly peaked $J(\mathbf{q})$ values at small \mathbf{q} :

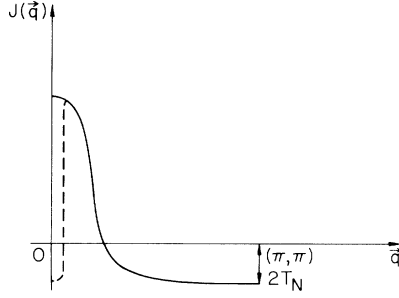


FIG. 2. Schematic view of the q -dependent exchange integral (Ref. 14) (solid line). The dashed line shows the reduction of the $q=0$ region in the presence of carriers.

$$J(\mathbf{q}=0) = \frac{V^4 a^2 m_0}{2\pi\Delta^2} \sim \frac{V^4}{\Delta^2 D}, \quad (5)$$

compared with

$$J(\mathbf{Q}_0) = -\frac{V^4 a^4 m_0^2}{2\pi^2 \Delta} \ln \left| \frac{D}{\Delta} \right| \sim -\frac{V^4}{\Delta D^2}. \quad (6)$$

[In what follows $\mathbf{Q}_0 = (\pi, \pi)$ and a is the elementary translation in the CuO_2 plane.]

One sees that the AF interaction is small, $|J(\mathbf{Q}_0)| \sim (\Delta/D)|J(0)|$, in the model. On the other hand, for small \mathbf{q} , the mean-field expression of the generalized susceptibility is rigorously justified:

$$\chi \propto \frac{1}{T + \frac{1}{2} J_{\text{eff}}(T, \mathbf{x}, \mathbf{q})}. \quad (7)$$

Here

$$J_{\text{eff}}(T, \mathbf{x}, \mathbf{q}) = J(T, \mathbf{x}, \mathbf{q}) + J_{\text{RKKY}}(T, \mathbf{x}, \mathbf{q}), \quad (8)$$

and $J_{\text{RKKY}}(\mathbf{q}, \mathbf{x}, T)$ is the contribution due to the pres-

$$J_{12}(\mathbf{q}) = -\frac{a^2 V_1^2 V_2^2 m_1 [A(\mu + \Delta_1)^2 + B(\mu + \Delta_1) + C]^{1/2}}{\pi(\mu + \Delta_1)C} + \frac{a^2 V_1^2 V_2^2 m_1 (AD_1^2 + BD_1 + C)^{1/2}}{\pi CD_1} + \frac{a^2 V_1^2 V_2^2 m_1 B}{2\pi C^{3/2}} \ln \left| \frac{2C^{1/2} [A(\mu + \Delta_1)^2 + B(\mu + \Delta_1) + C]^{1/2} / (\mu + \Delta_1) + 2C / (\mu + \Delta_1) + B}{2C^{1/2} (AD_1^2 + BD_1 + C)^{1/2} / D_1 + 2C / D_1 + B} \right|, \quad (9)$$

where

$$A = \left[1 + \frac{m_1}{m_2} \right]^2, \\ B = 2 \left[1 + \frac{m_1}{m_2} \right] \left[\varepsilon_{q_2} - \Delta_1 \frac{m_1}{m_2} - \Delta_2 \right] - 4\varepsilon_{q_2} \frac{m_1}{m_2},$$

and

$$C = \left[\varepsilon_{q_2} - \Delta_2 - \Delta_1 \frac{m_1}{m_2} \right]^2 + 4\Delta_1 \varepsilon_{q_2} \frac{m_1}{m_2}, \\ \varepsilon_{q_2} = \frac{q^2}{2m_2}.$$

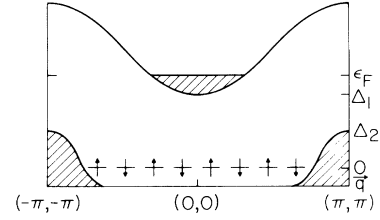


FIG. 3. Relative positions of the local levels and conduction bands. One band is completely filled up.

ence of holes in the conduction bands (for $q \sim 2p_F, R_0^{-1}$). The $J_{\text{eff}}(\mathbf{q})$ behavior is shown schematically along the Γ - X line in Fig. 2. The solid line in Fig. 2 represents long-range interaction in absence of holes; the dashed line shows the drastic reduction in J_{eff} at small \mathbf{q} by the RKKY contribution of 2D holes. The main shortcoming of the model is in the existence of a ferromagnetic instability at $\mathbf{q}=0$ due to this compensation. [Of course, the value of $J_{\text{eff}}(\mathbf{Q}_0)$ in Fig. 2 is related to the Néel temperature by the mean-field estimate only.] The static magnetic susceptibility in the paramagnetic phase increases with the hole concentration increase and with the decrease of temperature for this model.

Consider another model illustrated in Fig. 3. It contains now two itinerant zones. The first one is empty as above. The second band is completely filled up (by definition the local center is not able to accept more than one hole). However, even being occupied, the second band essentially contributes to the exchange interaction. In fact, if the local electron from a site i virtually goes to the first band (V_1), a hole from the second band could then replace it (V_2). Therefore, this mixed virtual process ($\propto V_1^2 V_2^2$) provides a new contribution to $J(\mathbf{q})$, which is most essential at $\mathbf{q} = \mathbf{Q}_0 = (\pi, \pi)$. The result for the two-dimensional case can be presented in the closed form

Here D_1, D_2 are the bandwidths and m_1, m_2 are the masses of the holes near the bottom of the first band and the top of the second band, correspondingly (both defined as positive here).

The chemical potential μ is proportional to the hole concentration x , namely,

$$x = \frac{m\mu a^2}{\pi}. \quad (10)$$

The explicit Eq. (9) is too cumbersome for a qualitative analyses. To make the formulas simpler, we shall further assume, in all the cases,

$$\Delta_{12} = \Delta_1 - \Delta_2 \ll \Delta, \quad \Delta_1 \approx \Delta_2 \approx \Delta.$$

Taking this limit for (9), one obtains

$$J(0) = \frac{V_1^4 a^2 m_1}{2\pi\Delta^2}, \quad (11)$$

$$J(\mathbf{Q}_0) = -\frac{a^2 V_1^2 V_2^2}{\pi\Delta^2} \frac{m_1 m_2}{m_1 + m_2} \left\{ \ln \left| \frac{\Delta(m_1 + m_2)}{\Delta_{12} m_2} \right| - 1 \right\}. \quad (12)$$

The view of $J(\mathbf{q})$ along the Γ - X line for this model is shown in Fig. 4. It is seen that the "staggered" part $J(\mathbf{q}=\mathbf{Q}_0)$, but also it provides a peaked interaction of the AF sign; i.e., the system of spins acquires a long-range AF interaction. [Actually, the very fact that $J(\mathbf{Q}_0)$ always possesses the correct (AF) sign is immediately seen from the general Eq. (4).] To illuminate the role of doping, we write down $J_{\text{eff}}(0)$ and $J_{\text{eff}}(\mathbf{Q}_0)$ in the presence of holes doped in the first band:

$$J(0) \approx -\frac{a^4 V_1^4 m_1^2}{2\pi^2 \Delta} \ln \left| \frac{D_1}{\Delta} \right| + \frac{a^4}{2\pi^2 \Delta} V_1^2 V_2^2 m_1 m_2 \ln \left| \frac{D_2}{\Delta} \right|, \quad (13)$$

$$J(\mathbf{Q}_0) \approx -\frac{a^2 V_1^2 V_2^2}{\pi\Delta^2} \frac{m_1 m_2}{m_1 + m_2} \times \left\{ \ln \left| \frac{\Delta(m_1 + m_2)}{\mu(m_1 + m_2) + \Delta_{12} m_2} \right| - 1 \right\}. \quad (14)$$

In Eqs. (13) and (14), μ is the chemical potential ($T=0$) of holes added into the central band. As for the static magnetic susceptibility, it has the same order of

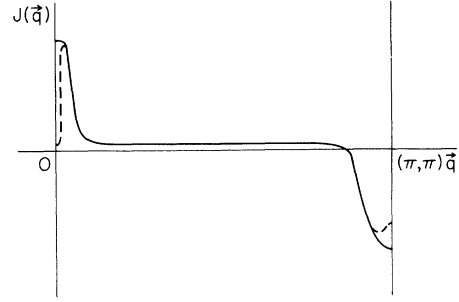


FIG. 4. $J(\mathbf{q})$ and $J_{\text{eff}}(\mathbf{q})$ for the model with one empty and one "filled-up" conduction band (solid and dashed lines, respectively). The incommensurate minimum near the (π, π) point can appear at finite hole concentration (see text).

magnitude as in Refs. 14 and 15 and approximately obeys the "Curie-Weiss behavior" $\chi \propto (T + \Theta)^{-1}$ with $\Theta \equiv \Theta(T, x)$:

$$\Theta = \frac{V^4 a^2 m_1}{4\pi\Delta^2} \exp \left[-\frac{\pi x}{a^2 m_1 T} \right] - \frac{a^4 V_1^4 m_1^2}{4\pi^2 \Delta} \ln \left| \frac{D}{\Delta} \right| + \frac{a^4}{4\pi^2 \Delta} V_1^2 V_2^2 m_1 m_2 \ln \left| \frac{D_2}{\Delta} \right|. \quad (15)$$

[In Eq. (15) we have neglected the contribution of holes thermally activated from the filled band.] Unlike Eq. (5), $J(0)$ in Eq. (15) has a positive sign. In addition to the above, Eq. (9) must be investigated with respect to peculiarities of the $J(\mathbf{Q})$ behavior near (π, π) : $\mathbf{Q} = \mathbf{Q}_0 + \mathbf{q}$. Namely, the exchange integral for small \mathbf{q} equals

$$J(\mathbf{Q}_0 + \mathbf{q}) \approx -\frac{a^2 V_1^2 V_2^2 m_1 m_2}{\pi\Delta^2 (m_1 + m_2)} \ln \left| \frac{2\Delta(m_1 + m_2)}{\mu(m_1 + m_2) + \Delta_{12} m_2 + [(m_2 - m_1)/(m_2 + m_1)]q^2 + u} \right|, \quad (16)$$

$$u = \{[\mu(m_1 + m_2) + \Delta_{12} m_2 + q^2/2]^2 - 2\mu q^2 m_1\}^{1/2}.$$

One sees, otherwise, that the "instability" [i.e., a maximum in $|J_{\text{eff}}(\mathbf{q})|$] may develop not at the commensurate vector \mathbf{Q}_0 , if only $m_1 > m_2$. The characteristic scale is

$$q_{\text{max}}^2 = 2 \{ [\Delta_{12} m_2 + \mu(m_2 - m_1)]^2 + \mu\Delta_{12}(m_1^2 - m_2^2) \}^{1/2} - 2m_2\Delta_{12} - 2\mu(m_2 - m_1). \quad (17)$$

(In all the expressions above, the isotropic masses m_1 and m_2 were considered.) Now we will discuss the last point. In any expression of the form of Eq. (7), the imaginary part in the denominator would appear as a result of the zone hole scattering process with a vector \mathbf{q} . Therefore, in the model of Fig. 3, there is no imaginary part in $\chi(\mathbf{q}, \omega)$ for $|\mathbf{q}| > 2p_F$ at $T < \Delta_{12}$. Any contribution into the NMR relaxation rate $T_1^{-1} \propto T \sum_{\mathbf{q}} \chi''(\omega, \mathbf{q})/\omega$ would be due to the small momenta contribution. We shall come back to this point in Sec. VIII.

IV. EMPTY BANDS AT THE BRILLOUIN-ZONE BOUNDARY

There are no changes if the positions of the filled and empty bands were interchanged, i.e., if the empty band were at the corner of the Brillouin zone (the point X) instead of being centered at the Γ point. A more peculiar situation arises if the empty bands are positioned, as shown in Fig. 5. There are now four terms contributing to the Heisenberg interaction in Eq. (6): $J_{11}(\mathbf{q})$, $J_{12}(\mathbf{q})$, $J_{22}(\mathbf{q})$, and $J_{21}(\mathbf{q})$. The first pair J_{11} , J_{22} are the exchange integrals for processes involving only one band (1 or 2). They behave as described in Sec. II and give rise to interaction peaked at the $\mathbf{q}=0$ point (in the absence of dopants). On the other hand, J_{12} , J_{21} are contributions from the two-band processes; their strengths are peaked at (π, π) . The Γ - X line scan for the interactions in this

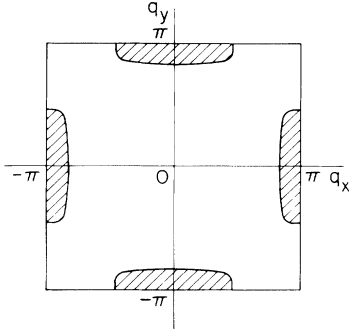


FIG. 5. Fermi surfaces for conduction bands at Brillouin-zone boundaries. The bands are related by the C_4 symmetry.

model is shown schematically in Fig. 6. As above, the solid line represents the long-range interaction in absence of holes, while the dashed line explicitly shows the reduction of J_{eff} near both the X and Γ points by added holes. The bands in this model are connected by rotational C_4 symmetry, and so they have the same hybridization and other parameters, and for isotropic spectrum the exchange integral has the same value at the X and Γ points. (This would be not valid for a nonspherical shape of the energy surfaces.) Without doping the maximum values of exchange interactions are again at the X and Γ points and with a shallow minimum at F points [$F=(0, \pi)$, $F'=(\pi, 0)$]:

$$J(0,0) = J(\pi, \pi) = \frac{V^4 a^2 m}{\pi \Delta^2}, \quad (18)$$

$$J(0, \pi) = J(\pi, 0) = -\frac{2V^4 a^4 m^2}{\pi^2 \Delta} \ln \left| \frac{D}{\Delta} \right|. \quad (19)$$

Therefore, in absence of holes, for this band structure, $J(\pi, \pi)$ would have a "wrong" sign: $J(\pi, \pi)$ is big but positive! When even an insignificant amount of carriers is introduced into the system, the exchange integral would change drastically in the vicinity ($\delta q \approx 2p_F$) of both the Γ and X points, so that

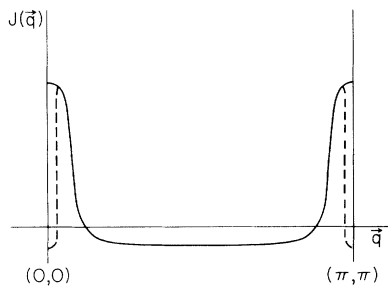


FIG. 6. \mathbf{q} dependence of $J(\mathbf{q})$ and $J_{\text{eff}}(\mathbf{q})$ for the model shown in Fig. 5 (the solid and dashed lines, respectively). $J_{\text{eff}}(\mathbf{q})$ differs from $J(\mathbf{q})$ only in the narrow range ($\Delta a \sim 2p_F$) near the X and Γ points.

$$J(0,0) = J(\pi, \pi) = -\frac{2V^4 a^2 m^2}{\pi^2 \Delta} \ln \left| \frac{D}{\Delta} \right|. \quad (20)$$

That is, the commensurate exchange integrals decrease by the factor Δ/D . The AF and ferromagnetic instabilities would compete in the presence of dopants at lower temperatures. The temperature and concentration dependence of the static magnetic susceptibility [and $\chi(\pi, \pi)$] would again be given by Eq. (6), where $J_{\text{eff}}(x, T)$ is the value of the exchange integral at the Γ point:

$$J_{\text{eff}}(x, T) = \frac{V^4 a^2 m}{\pi \Delta^2} \exp \left[-\frac{\pi x}{a^2 m T} \right] - \frac{2V^4 a^4 m^2}{\pi^2 \Delta} \ln \left| \frac{D}{\Delta} \right|. \quad (21)$$

So, once again, the static susceptibility in the paramagnetic phase increases with the temperature decrease and concentration increase. Note the small values of $J(0, \pi)$ [compared with Eq. (18)] or J_{eff} at "low temperature." The problem of whether the system would await until a commensurate instability takes place at low temperatures or, whether instead, some other ordering is possible for the long-range interaction of Eqs. (18) and (19) deserves a separate discussion.

Coming back to the measurements of the relaxation rate in the NMR or neutron experiments, one sees that an imaginary part in the denominator of Eq. (7) would come from electron scattering at the vector \mathbf{q} . Unlike the single empty-band picture, now there is a contribution near the (π, π) point which is exclusively due to the existence of the two pieces of the Fermi surface. Namely, the imaginary part in the denominator of Eq. (7) is given by

$$J''(\mathbf{q}, \omega) = -\sum_i \frac{a^2 \omega V^4}{4\pi v_{1i} v_{2i} \sin(\theta_i) \Delta^2}. \quad (22)$$

Here v_1, v_2 are the Fermi velocities at points i , where the energy conservation law is obeyed and the sum is taken over all such points; θ_i is the angle between the two velocities there. So the imaginary contribution from the electron scattering is now of the order of $\sim (\omega/\mu) V^4 / \Delta^2 D$. Note that this contribution is sharply peaked by itself on the scale $q \approx 2p_F$ in the vicinity of the Γ and X points.

V. TWO EMPTY BANDS

Consider next the model shown in Fig. 7. This model contains two empty bands, and both bands in no way are related due to any symmetry. So they may have completely independent parameters. However, some of the properties of this model remain similar to those of the model of Sec. IV. Thus the exchange interaction consists again of the four contributions J_{11}, J_{22}, J_{12} , and J_{21} . The first pair of those is peaked near the Γ point, while the second pair is peaked near the X point. The new values of $J(\mathbf{q})$ near the peak positions are, however, different primarily because of the difference in the hybridization parameters (Fig. 8):

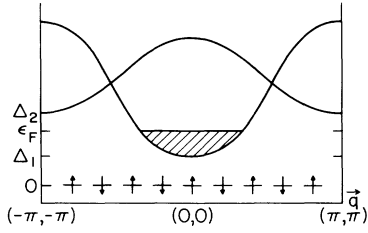


FIG. 7. Model with two arbitrary empty bands.

$$J(0,0) \simeq \frac{V_1^4 a^2 m_1}{2\pi\Delta^2} + \frac{V_2^4 a^2 m_2}{2\pi\Delta^2}, \quad (23)$$

$$J(\pi, \pi) = \frac{a^2 V_1^2 V_2^2}{\pi\Delta^2} \frac{m_1 m_2}{m_1 - m_2} \ln \left| \frac{m_1}{m_2} \right|. \quad (24)$$

From Eq. (24) one easily sees that the sign of $J(\pi, \pi)$ does not depend on the choice of masses; it is always positive. Once again, the exchange integral has a broad minimum at the F point:

$$\begin{aligned} J(0, \pi) &= J(\pi, 0) \\ &= -\frac{a^4 V_1^4 m_1^2}{2\pi^2 \Delta} \ln \left| \frac{D_1}{\Delta} \right| - \frac{a^4 V_2^4 m_2^2}{2\pi^2 \Delta} \ln \left| \frac{D_2}{\Delta} \right| \\ &\quad - \frac{a^4 V_1^2 V_2^2 m_1 m_2}{2\pi^2 \Delta} \ln \left| \frac{D_1 D_2}{\Delta^2} \right|. \end{aligned} \quad (25)$$

The drastic compensation for the exchange integrals at the Γ and X points takes place again when both bands contain holes. New options occur because one band can start to be filled first (as in Fig. 7). In this case the compensation of $J(\mathbf{q})$ in the presence of dopants does not yield either AF or ferromagnetic instabilities: The values of exchange integral remain positive:

$$J(0,0) \simeq \frac{V_2^4 a^2 m_2}{2\pi\Delta^2}, \quad (26)$$

$$J(\pi, \pi) \simeq \frac{a^2 V_1^2 V_2^2}{\pi\Delta^2} \frac{m_1 m_2}{m_1 - m_2} \ln \left| \frac{\Delta_{12} m_1}{\mu(m_2 - m_1) + \Delta_{12} m_2} \right|. \quad (27)$$

The inverse static magnetic susceptibility for this case equals

$$\chi^{-1}(\mathbf{x}, T) \propto T + \frac{J_{\text{eff}}(\mathbf{x}, T)}{2} = T + \frac{J_{11}(\mathbf{x}, T) + J_{22}(\mathbf{x}, T)}{2}. \quad (28)$$

The second term in this expression could, in principle, simulate an increase of the magnetic susceptibility as the temperature increases. However, this would be the result of the thermal activation of holes into the second conduction band, which is possible, of course, only under rather specific assumptions; namely, (1) $J_{11}(\mathbf{x}, T)$ must be small enough. This could be the case assuming $V_1 \ll V_2$. (2) The bottoms of the two bands must be near on the scale

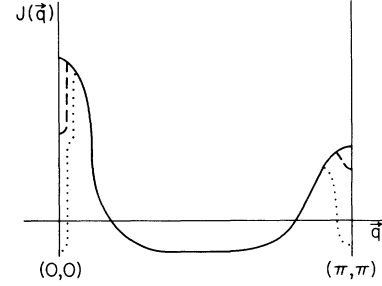


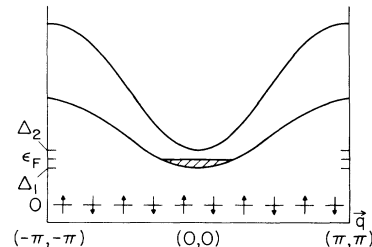
FIG. 8. \mathbf{q} dependence of exchange integral for the model with two “empty” bands: no holes are present, solid line; the lower band is partially filled, the dashed curve; and both bands become partially filled, the dotted curve.

of temperature. As soon as the Fermi level reaches the bottom of the second band, both the AF and ferromagnetic instabilities arise (at low T) and the situation becomes quite similar to the one considered in Sec. IV, namely, that the same type of drastic compensation appears in a small vicinity of X and Γ points:

$$\begin{aligned} J(0,0) &= J(\pi, \pi) \\ &= -\frac{a^4 V_1^4 m_1^2}{2\pi^2 \Delta} \ln \left| \frac{D_1}{\Delta} \right| - \frac{a^4 V_2^4 m_2^2}{2\pi^2 \Delta} \ln \left| \frac{D_2}{\Delta} \right| \\ &\quad - \frac{a^4 V_1^2 V_2^2 m_1 m_2}{2\pi^2 \Delta} \ln \left| \frac{D_1 D_2}{\Delta^2} \right|. \end{aligned} \quad (29)$$

The contribution to the imaginary part itself is peaked near Γ point if only one band is filled, while if the two bands become occupied, a nonzero contribution near (π, π) vector appears from the electron process on different pieces of the Fermi surface. This contribution is again described by Eq. (22). Thus there is no imaginary part $\chi''(\mathbf{q}, \omega)$ for $q > 2 \max\{p_{F1}, p_{F2}\}$ and $|\mathbf{q} - \mathbf{Q}_0| > \{p_{F1} + p_{F2}\}$. The contribution into $\chi''(\mathbf{q}, \omega)$ near the X point appears at finite concentration, i.e., only when both bands become partially occupied.

For completeness, we consider the case of two conduction bands centered at the X point (Fig. 9). The exchange integral again consists of the four contributions: J_{11} , J_{12} , J_{21} , and J_{22} . However, all of them have peaks at the Γ point only and much less minima at the AF wave vectors, so that the resulting exchange integrals at these point are

FIG. 9. Two empty bands centered at the Γ point.

characterized by the values

$$J(0,0) \simeq \frac{V_1^4 a^2 m_1}{2\pi\Delta^2} + \frac{V_2^4 a^2 m_2}{2\pi\Delta^2} + \frac{a^2 V_1^2 V_2^2}{\pi\Delta^2} \frac{m_1 m_2}{m_1 - m_2} \ln \left| \frac{\Delta_{12} m_1}{\mu(m_2 - m_1) + \Delta_{12} m_2} \right|, \quad (30)$$

$$J(\pi,\pi) = -\frac{a^4 V_1^4 m_1^2}{2\pi^2 \Delta} \ln \left| \frac{D_1}{\Delta} \right| - \frac{a^4 V_2^4 m_2^2}{2\pi^2 \Delta} \ln \left| \frac{D_2}{\Delta} \right| - \frac{a^4 V_1^2 V_2^2 m_1 m_2}{2\pi^2 \Delta} \ln \left| \frac{D_1 D_2}{\Delta^2} \right| \quad (31)$$

[i.e., $J(\pi,\pi) \simeq (\Delta/D)J(0,0)$].

As the first band starts to fill up, a sharp local minimum appears at the ferromagnetic wave vector. However, ferromagnetic instability does not develop until both bands are filled. The Γ - X line behavior for the interaction $J(\mathbf{q})$ in this model is shown in Fig. 10. The temperature dependence of the magnetic susceptibility is determined by the sum of four contributions. Once again, an increase of static magnetic susceptibility with the temperature increase can be obtained only within frameworks of special assumptions already indicated above. The imaginary part of the generalized magnetic susceptibility is, of course, concentrated near the $\mathbf{q}=(0,0)$ point.

To complete this section, we shall mention briefly the possibility that the Fermi surfaces are of the form shown in Fig. 11. Once again, there are no symmetry arguments as to why the zones would be located at these points. The above calculations can be easily repeated. However, such Fermi surfaces usually appear in the literature for other reasons (see Ref. 21), such as in the "spin-bag" picture²² for superconductivity if the nesting features of the "bare" Fermi surface serve implicitly as the reason underlying the tendency to antiferromagnetic ordering. In this case one often departs from the tight-binding square bare Fermi surface. Regarding the doping procedure, there are two alternatives. The open parts of the Fermi surface in Fig. 11 may be the result of an incomplete "nesting" of the bare metallic electron Fermi surface and, hence, are

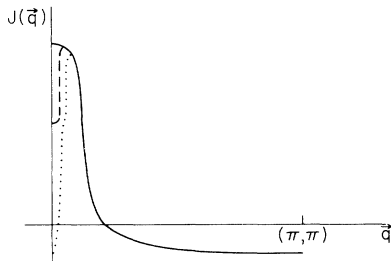


FIG. 10. \mathbf{q} behavior of $J(\mathbf{q}), J_{\text{eff}}(\mathbf{q})$ in the model shown in Fig. 9: empty bands, the solid line; one band is partially filled, the dashed line; and both bands become filled by holes, the dotted line.

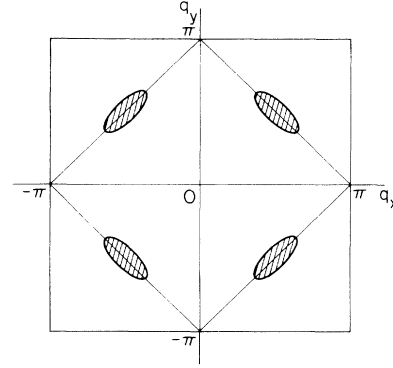


FIG. 11. Fermi surfaces in the "nesting" picture.

not too sensitive to doping. In any case the presence of such pockets would result in a metal-like conductivity at higher temperatures without doping. This is, probably, not the case for the low-doped members of the 2:1:4 family.

On the other hand, the "spin gap" can already be well developed, as in Ref. 22, so that all bare electrons are deeply under the gap. Then the added holes come into the new "conduction band" (i.e., above the gap), where they now experience a strong interaction with the two-dimensional spin-density-wave (SDW) fluctuations. The "conduction-band minima" could be now positioned not only as shown in Fig. 11, but may bend the points shown in Fig. 5 as well.^{22,33} In any event there are no local moments in this itinerant scheme, and the authors are not aware of a comprehensive quantitative study of the consequences of this approach to the interpretation of recent NMR data.

VI. IMAGINARY PART OF THE MAGNETIC SUSCEPTIBILITY

Above we have already had a number of chances to indicate that, in general, the peculiarities of the imaginary part of the magnetic susceptibility would strongly depend on assumptions for the hole energy spectrum. In this section we shall add some comments of a more general character in this connection.

The neutron experiments measure directly only $\chi''(\mathbf{q}, \omega)$. Fortunately enough, in the case of $\text{La}_{2-x}\text{Sr}_x\text{CuO}_4$, it is well known that pure La_2CuO_4 becomes antiferromagnetically ordered below $T_N \sim 300$ K and that the 2D coherence length $\zeta(T)$, as measured by neutron inelastic scattering,²⁵ is large and remains strongly temperature dependent at higher temperatures, even if a small amount of the strontium ions is added. In other words, the presence of local moments is well documented on the scale of small x (see also results of the μ^+ SR study in Ref. 24). In the metallic regime (from the side of $\text{La}_{1.85}\text{Sr}_{0.15}\text{CuO}_4$), the Fermi-liquid approach seems to be more appropriate. Meanwhile, even in this case, the MMP analyses of the NMR data¹⁰ are unambiguously in favor of the important role of antiferromagnetic fluctuations. However, while at very small dopant

concentrations the relaxation [i.e., $\chi''(\mathbf{q}, \omega)$] is due to some kind of spin-spin interactions that would be the only source of the dissipation in insulating antiferromagnets, in the metallic regime the conduction-hole contribution dominates, as it is clearly seen, from the sharp decrease of the relaxation rate $T_1^{-1}(T)$ below the superconducting transition.⁸

In accordance with Eq. (7), we write down the generalized susceptibility in the form

$$\chi^{-1}(\mathbf{q}, \omega) \propto T + \Theta(\mathbf{q}, \omega, T) + V_{sd}^2 \Pi_0(\mathbf{q}, \omega, T), \quad (32)$$

where $\Pi_0(\mathbf{q}, \omega, T)$ is the ordinary Fermi-liquid contribution, if this exists. Making no special assumption now that the Fermi surfaces are somehow small, let us concentrate some rather trivial features of the imaginary part $\Pi_0''(\mathbf{q}, \omega, T)$:

$$\Pi_0(\mathbf{q}, \omega, T) = \Pi_0'(\mathbf{q}, \omega, T) + i\Pi_0''(\mathbf{q}, \omega, T). \quad (33)$$

At an arbitrary shift (an arbitrary \mathbf{q} vector), $\Pi_0''(\mathbf{q}, \omega, T)$ is given by Eq. (22), which we rewrite omitting the coefficient responsible for the coupling between "localized" and "delocalized" electrons:

$$\Pi_0''(\mathbf{q}, \omega, T) \propto -\omega \sum_i \frac{1}{v_{1i} v_{2i} \sin(\theta_i)}. \quad (34)$$

In Eq. (34) there is no temperature or frequency dependence. This is correct until $\sin(\theta_i) \neq 0$. When the Fermi-surface shift along the \mathbf{q} direction reaches the value of the corresponding Kohn anomaly, $\Pi_0''(\mathbf{q}, \omega, T)$ acquires the form

$$\begin{aligned} & \frac{a^2 p_1 p_2}{4\sqrt{2}\pi v_1 v_2 (p_1 + p_2)} \\ & \times \int_{-\infty}^{+\infty} \left[\tanh \frac{\varepsilon}{2T} - \tanh \frac{\varepsilon + \omega}{2T} \right] \\ & \times \frac{\{B(\varepsilon) + [(A/\tau)^2 + B(\varepsilon)^2]^{1/2}\}^{1/2}}{[(A/\tau)^2 + B(\varepsilon)^2]^{1/2}} d\varepsilon. \end{aligned} \quad (35)$$

Here

$$\begin{aligned} A &= \frac{p_1 p_2 (v_1 + v_2)}{(p_1 + p_2) v_1 v_2}, \\ B(\varepsilon) &= \frac{2p_1 p_2}{p_1 + p_2} \left[\frac{\varepsilon}{v_1} + \frac{\varepsilon + \omega}{v_2} + \delta_q \right], \end{aligned}$$

where $p_{1,2}$ are the momenta values and $v_{1,2}$ are the velocities on the opposite sides of the Fermi surface across the \mathbf{q} vector and $\delta_q = q - q_0$ characterizes how close is \mathbf{q} to its Kohn-anomaly value. Equation (35) has been obtained making use of the fact that, experimentally, $1/\tau = \alpha T$;

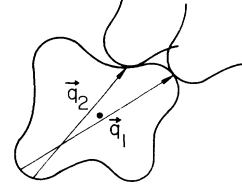


FIG. 12. Schematic view showing that the Kohn anomaly in $\chi''(\mathbf{q}, T, \omega)$ would vary with the direction of the \mathbf{q} vector.

i.e., the scattering dependence is due to a quasielastic contribution.

Comparing Eq. (35) with Eq. (34), it is seen that there is an enhancement in the vicinity of the Kohn anomaly for the imaginary part $\chi(\mathbf{q}, \omega, T)$, and this enhancement reaches the order of $[\varepsilon_F / \max(1/\tau, \delta_q v)]^{1/2}$ at small ω :

$$\begin{aligned} & -\frac{a^2 (v\tau p)^{1/2} \omega}{8\sqrt{2}\pi v_1 v_2 T} \\ & \times \int_{-\infty}^{+\infty} \cosh^{-2} \left\{ \frac{\varepsilon}{2T} \right\} \\ & \times \frac{\{2\tau(\varepsilon + \delta_q v) + [1 + 4\tau^2(\varepsilon + \delta_q v)^2]^{1/2}\}^{1/2}}{[1 + 4\tau^2(\varepsilon + \delta_q v)^2]^{1/2}} d\varepsilon. \end{aligned} \quad (36)$$

[Here $v = v_1 v_2 / (v_1 + v_2)$ and $p = p_1 p_2 / (p_1 + p_2)$.] First, the shape of the anomaly [Eq. (36)] is asymmetric in its δ_q dependence along the \mathbf{q} direction (if $|\delta_q v| > 1/\tau$). Second, the result of Eq. (36) is temperature dependent since $1/\tau \propto T$. For the NMR experiments this anomaly is integrated over momenta in the expressions for the relaxation rate and would probably result in a numerical correction to $T_1^{-1}(T)$ in the MMP calculations. However, the Kohn anomaly should be seen in the neutron inelastic experiments. A more attentive look at Eq. (35) discloses that $\chi''(\mathbf{q}, \omega, T)$ is actually both frequency and temperature dependent on the scale $\omega \propto 1/\tau \propto T$. As was already pointed out, $\chi''(\mathbf{q}, \omega, T)$ is asymmetric along a given direction (\mathbf{q}) when passing through the Kohn-anomaly point, and in addition, the value of the anomaly of Eq. (36) varies with the direction of the \mathbf{q} vector, reflecting, basically, the change in the curvature of the Fermi surface as it is scanned by the given \mathbf{q} . The option of relating the incommensurabilities around $\mathbf{Q}_0 = (\pi, \pi)$ observed in Ref. 20 with the Fermi surface features and their dependence on concentration of strontium, while being very tempting, remains unresolved, so far. However, depending on the improvement of the experimental facilities, Eq. (36) could become an important check for the Fermi-liquid picture. To conclude, we once again would like to emphasize the asymmetry of the linewidth when measured along a fixed \mathbf{q} direction. The sensitivity of Eq. (35) to the choice of the \mathbf{q} scan is shown schematically in Fig. 12 for an arbitrary Fermi-surface shape which has the Kohn vectors close enough to $\mathbf{q} = \mathbf{Q}_0 = (\pi, \pi)$.

VII. DISCUSSION

Coming back to the problem of how the metallic and insulating regimes can merge with a change in the dopant concentration, as was posed in the Introduction, it is appropriate now to discuss again the difference expected between $\text{La}_{2-x}\text{Sr}_x\text{CuO}_4$ and $\text{La}_2\text{CuO}_{4+\delta}$. For the latter compound the first-order phase transition takes place when the oxygen is dissolved and is accompanied by a spatial phase separation due to high enough oxygen mobility, while in the former case the strontium ions are not mobile at these temperatures. It is important, however, that the so-called "oxygen-rich" phase of La_2CuO_4 correspond, as estimated, to $\delta \approx 0.08$; i.e., the oxygen concentration remains rather low even in the "metallic" phase. Therefore the increase of δ results in an abrupt but somehow minor change of the overall lattice structure.

For the former compound, where strontium atoms are already fixed at room temperature, the concentration increase would, probably, mean the gradual passage through the phase separation region. Experimentally, this passage would be a well-determined conventional route, provided that samples of $\text{La}_{2-x}\text{Sr}_x\text{CuO}_4$ are prepared in the most homogeneous fashion. (The uncontrolled variation in the oxygen content can provide a coexistence of two phases.²⁵) If the point of view is accepted that all changes at small concentrations exert an influence on the properties of the conducting CuO_2 plane only, a mapping between strontium- and oxygen-"doped" metallic states is expected. The correspondence follows the average distance between introduced defects (Sr or O). This concept²⁶ has strong support in the fact that in the cases of both enriched $\text{La}_2\text{CuO}_{4.03}$ and "optimal" $\text{La}_{1.85}\text{Sr}_{0.15}\text{CuO}_4$ the temperatures of the superconducting transition practically coincide.

On the other hand, it is known that the Hall coefficient $R_H(x)$ behaves as $R_H \propto x^{-1}$ for $\text{La}_{2-x}\text{Sr}_x\text{CuO}_4$ (and is temperature independent) at $x < 0.1$ (see Ref. 18 for the review), and this is the most serious evidence in favor of the concept where carriers are doped into a sort of conduction band. Hence we must now decide which of the various possibilities for the energy spectrum enumerated above is compatible with the properties of $\text{La}_{2-x}\text{Sr}_x\text{CuO}_4$. It is worth emphasizing once again that in no case were our approximations, made above ($\Delta \ll D$), considered as a quantitative statement. They have been introduced to exaggerate the point, for instance, that spin interactions are never restricted by nearest neighbors only. These assumptions are also helpful in understanding the relative importance for the ferromagnetic and antiferromagnetic regions of the wave vectors in the spin-spin interactions in a more controllable way. An obvious artifact of the model is the extreme sensitivity of interactions for the ferromagnetic and antiferromagnetic wave vectors to the dopant concentration at some special choices of the energy spectrum (see Fig. 2 and Secs. IV and V). The sensitivity is merely due to the fact that the exchange-spin interaction involves the virtual excitation of electrons across the gap in the narrow range of these specific wave vectors. This range rapidly becomes unavailable when additional holes are added

into conduction bands. The effects would be much weaker but nevertheless still present, if some narrow conduction bands were chosen.

Reviewing the above results, we conclude that among the variety of band positions investigated in previous sections, there is the only option which seems to be consistent with what is known about the basic properties of $\text{La}_{2-x}\text{Sr}_x\text{CuO}_4$. Indeed, pure La_2CuO_4 is a 3D antiferromagnet below $T_N \sim 300$ K and is in the strongly developed antiferromagnetic fluctuation regime at temperatures well above room temperature.²³ One sees that only the band structure of Sec. IV provides the exchange component for the antiferromagnetic vector which has the correct sign. [We digress from a possibility that the antiferromagnetic ordering is due to smaller (in Δ/D) contributions, which can be considered, as in Refs. 14 and 15, in the mean-field approach only.] The advantage of Eqs. (9)–(13) is also that $J(\pi, \pi)$ is now quite stable in the presence of holes gradually decreasing with the dopant concentration increase.

The above analysis was applicable in the paramagnetic phase. None of the expressions for the paramagnetic susceptibility $\chi(0, x, T)$ obtained before would be capable of reproducing the remarkable fact that in $\text{La}_{2-x}\text{Sr}_x\text{CuO}_4$, at least for $x < 0.10$, $\chi(T)$ monotonically increases with the increase of temperature up to 1000 K,^{27,28} except the region where the three-dimensional Néel transition takes place (at low strontium concentrations). It is also seen from the data^{27,28} that at higher x , $x \geq 0.1$, a gentle maximum appears, which apparently shifts toward lower temperatures with the further increase of x . (The data^{27,28} do not agree numerically, but show the same tendency.)

There exists a commonly accepted experimental estimate for the exchange-integral value J in La_2CuO_4 obtained both from neutron-²⁹ and Raman-scattering measurements:^{30,31} $J \sim 0.1$ eV. Hence the growth of Néel-type ordering should start in the temperature range where samples are actually synthesized. Then there is no space for the paramagnetic phase. The fluctuation regime at lower temperatures is already strongly developed, manifesting a paramagnon-type of spin dynamics.²⁹ The sensitivity of the Néel temperature to the doping process at very small concentration is usually described in terms of static defects which destroy the three-dimensional Néel ordering. In the range of concentrations where $R_H(x) \sim x^{-1}$, it seems plausible to use the concept of conduction-band doping. As mentioned in Ref. 14, 3D Néel ordering would be then destroyed in this model by formation of large 2D magnetic polarons. (The polaron size would, actually, be determined by the Coulomb size of hole orbits.)

A few words concerning the conductivity in these compounds are in order. The resistivity data at low concentrations are usually not well reproducible. An important feature, however, is the presence of some traps in the samples with poor concentration, which is seen at low temperatures as Mott's "variable-range hopping" behavior: $\ln[\rho(T)] \propto (T_0/T)^{1/4}$. The large typical values of $T_0 \sim 10^5$ – 10^6 K show that there is actually a large number (more precisely, the density of states is large) of

“traps” at the Fermi level. It is not clear how it can be understood in the above picture. However, very soon (with the concentration and temperature increase) the delocalized component in the conductivity arises, which is responsible for the metallic type of behavior. Then any band picture for the conduction electrons is consistent with the basic transport properties, while the tendency to antiferromagnetism is described in the framework of the energy spectrum of Sec. IV. Materials are conductors because of presence of dopants, but the role of disorder is still not quite clear.

The increase (above $x > 0.1$) of the strontium concentrations is characterized by the deviation of $R_H(x)$ from x^{-1} behavior, and in addition, the Hall coefficient begins to depend on temperature.³² As has been repeatedly stressed above, the increase of strontium content, even if samples are “homogeneous,” is not a thermodynamical equilibrium path: the energy spectrum is gradually changed by the external source. Regarding the model of Sec. IV, it is tempting to relate the above change in Hall-coefficient behavior with the motion of the upper (conducting) and the lower (filled-up) bands toward each other, which would result eventually in the opening of electron-hole pockets. Whether the localized levels stay apart or whether their energy position mixes with the conduction band is far from being clear, and we shall not make speculations about it. In any event the crossing of the two bands could model the phase transition between the two phases of $\text{La}_2\text{CuO}_{4+\delta}$, providing a mapping between both compounds in terms of changes in their energy spectrum. It has also been reported⁷ that the further increase of the Sr- concentration suppresses the superconducting phase, while the ground state remains metallic. A possibility for understanding this mechanism in the framework of this model has already been suggested in Ref. 15.

In conclusion of this section, we shall once again point out that for the above model the electron correlations were needed to provide the localized moments. In terms of the Hubbard model, the oxygen orbitals are responsible for the formation of the band which has the role of the “upper” Hubbard band where holes can now go. (So the Hubbard repulsion was taken as infinite.) The exchange interaction for the localized moments is therefore determined in an independent fashion. The paramagnetic phase is, probably, never seen in the 2:1:4 compounds at small x . Instead, 2D magnetic fluctuations start immediately to grow. The monotonous decrease of $\chi_0(T)$ with the temperature decrease is a signature for $\text{La}_{2-x}\text{Sr}_x\text{CuO}_4$ (for $x < 0.1$) the fluctuations are already in the nonlinear regime³³ (i.e., the room-temperature interval lies somehow far below the mean-field Néel temperature), unlike as was assumed in Ref. 10 for metallic $\text{La}_{1.85}\text{Sr}_{0.15}\text{CuO}_4$. (For the long-range AF interaction, understanding, in terms of the modules of the spin order parameter and spin phase fluctuations, is possible.)

The AF order would double the lattice cell, making points Γ and X in Fig. 3 equivalent. As a result, the hole energy spectrum becomes similar to the one for the Hubbard model. The correspondence with the results of Refs. 22 and 33 becomes clearer starting from the side of the

weak-coupling limit when the magnetic phase arises as a result of nesting features of the Fermi surface for the itinerant electrons. If the commensuration energy for the SDW exceeds an imperfect Fermi-surface nesting, the resulting spectrum is characterized by the gap between filled-up valence and conduction bands where dopants can be added. Practically, most of the configurations for the zone bands considered above are also possible in the SDW picture. The crucial difference between the results of Refs. 22 and 33 and the model above lies in the assumption that the “gap” between valence and conduction bands is in our case due to the presence of the “oxygen orbital” contribution, while in the SDW picture the gap is the measure of the strength of a spin order parameter. Second, in our model, the moments are localized. The spin-exchange interaction is expressed in terms where the Hubbard repulsion U does not appear at all and was taken as $U \rightarrow \infty$.

VIII. SUMMARY

We have investigated a number of zone bands and their combinations for the conduction-hole spectrum. The band structure shown in Fig. 3 is singled out by the fact that it describes the tendency to AF ordering in our system. We have seen that the imaginary part of the magnetic susceptibility $\chi''(\mathbf{q}, \omega, T)$ —more precisely, its hole component—would be absent at a small concentration of the AF range of \mathbf{q} vectors. Hence the latter should be due to a spin-relaxation mechanism. If, however, the picture of transition to the metallic regime suggested above were correct, the hole contribution at $\mathbf{q} \simeq (\pi, \pi)$ appears and should become overwhelming at low temperatures. The decrease of the static magnetic susceptibility with the temperature decrease, in our opinion, can be ascribed exclusively to the growth of a magnetic order, in a form of growing fluctuations or some magnetic transition. (The model with long-range interactions by itself also provides a scheme for more exotic magnetic states.) In the well-developed metallic regime, the magnetic fluctuations, as seen by neutrons, would reveal Kohn-like anomalies associated with the Fermi-surface shape. The large value of $J \sim 0.1$ eV, as found experimentally, implies that, if applied to actual materials, the model parameters V , Δ , and D are approximately of the same scale.

ACKNOWLEDGMENTS

The authors are especially grateful to D. Pines, discussions who stimulated our interest in understanding the above problems. The useful comments and numerous discussion on the physics of the problem are acknowledged with gratitude to Z. Fisk, D. Ginsberg, T. Imai, J. Jorgensen, J. R. Schrieffer, and C. Slichter. This work was supported by the Science and Technology Center for Superconductivity under NSF Grant No. DMR88-09854 and (V.B.) by a grant from the John D. and Catherine T. MacArthur Foundation.

- ¹In the "1:2:3"-based materials, the problem is more obscured by the presence of two CuO₂ planes (and CuO₂ chains).
- ²B. Dabrowski, J. D. Jorgensen, D. G. Hinks, S. Pei, D. R. Richards, H. B. Vanfleet, and D. L. Decker, *Physica C* **162-164**, 99 (1989).
- ³C. Chaillout, J. Chenavas, S-W. Cheong, Z. Fisk, M. S. Lehmann, M. Marezio, B. Morosin, and J. E. Schirber, *Physica C* **162-164**, 57 (1989).
- ⁴C. Chaillout, J. Chenavas, S-W. Cheong, Z. Fisk, M. Marezio, B. Morosin, and J. E. Schirber, *Physica C* **170**, 87 (1990).
- ⁵M. F. Hundley, J. D. Thompson, S. W. Cheong, Z. Fisk, and J. E. Schirber, *Phys. Rev. B* **41**, 4062 (1990).
- ⁶J. D. Jorgensen, P. Lightfoot, Shiyon Pei, B. Dabrowskii, D. R. Richards, and D. G. Hinks, in *Advances in Superconductivity*, edited by K. Kajmura and H. Haekawa (Springer-Verlag, Tokyo, 1991), Vol. III, p. 337.
- ⁷J. B. Torrance, Y. Tokura, A. I. Nazzal, A. Bezing, T. C. Huang, and S. S. P. Parkin, *Phys. Rev. Lett.* **61**, 1127 (1988). See also J. Torrance and R. Cava (unpublished).
- ⁸C. H. Pennington and C. P. Slichter, in *Physical Properties of High Temperature Superconductors*, edited by D. Ginsberg (World Scientific, Singapore, 1990), Vol. II, p. 269.
- ⁹A. J. Millis, H. Monien, and D. Pines, *Phys. Rev. B* **42**, 167 (1990).
- ¹⁰H. Monien, P. Monthoux, and D. Pines, *Phys. Rev. B* **43**, 275 (1991).
- ¹¹F. Mila and T. M. Rice, *Physica C* **157**, 561 (1989).
- ¹²T. Imai, K. Yoshimura, T. Uemura, H. Yasuoka, and K. Kosuge, *J. Phys. Soc. Jpn.* **59**, 3846 (1990).
- ¹³L. P. Gor'kov and A. V. Sokol, *Pis'ma Zh. Eksp. Teor. Fiz.* **46**, 333 (1987) [*JETP Lett.* **46**, 420 (1987)]; [**48**, 547 (1988)].
- ¹⁴L. P. Gor'kov and A. V. Sokol, *J. Phys. (Paris)* **50**, 2823 (1989).
- ¹⁵L. P. Gor'kov and A. V. Sokol, *Physica C* **159**, 329 (1989).
- ¹⁶C. M. Varma, S. Schmitt-Rink, and E. Abrahams, in *Novel Superconductivity*, edited by S. A. Wolf and V. Z. Kresin (Plenum, New York, 1987), p. 355.
- ¹⁷K. Levin, J. H. Kim, J.-P. Lu, and Q. M. Si, *Physica C* **175**, 449 (1991).
- ¹⁸N. P. Ong, in *Physical Properties of High Temperature Superconductors* (Ref. 8), Vol. II, p. 459.
- ¹⁹L. P. Gor'kov, *Physica C* **162-164**, 12 (1989).
- ²⁰S-W Cheong, G. Aeppli, T. E. Mason, H. Mook, S. M. Hayden, P. C. Canfield, Z. Fisk, K. N. Clausen, and J. L. Martinez, *Phys. Rev. Lett.* **67**, 1791 (1991).
- ²¹P. A. Lee, the review paper in *Proceedings of the Los Alamos Symposium on High Temperature Superconductivity*, edited by K. S. Bedell, D. Coffey, D. E. Heltser, D. Pines, and J. R. Schrieffer (Addison-Wesley, Redwood City, CA, 1990), p. 103.
- ²²J. R. Schrieffer, X. G. Wen, and S. C. Zhang, *Phys. Rev. Lett.* **60**, 944 (1988); *Phys. Rev. B* **39**, 11 663 (1989).
- ²³K. Yamada, K. Kakurai, Y. Endoh, T. R. Thurston, M. A. Kastner, R. J. Birgeneau, G. Shirane, Y. Hidaka, and T. Murakami, *Phys. Rev. B* **40**, 4557 (1989).
- ²⁴D. R. Harshman, G. Aeppli, B. Batlogg, G. P. Espinosa, R. J. Cava, A. S. Cooper, L. W. Rupp, E. J. Ansaldo, and D. L. Williams, *Phys. Rev. Lett.* **63**, 1187 (C) (1989).
- ²⁵M. A. Kennard, Y. Q. Song, K. R. Poepplmeier, and W. P. Halperin, *Chem. Mater.* **3**, 672 (1991).
- ²⁶V. A. Borodin, L. P. Gor'kov, F. F. Igoshin, P. A. Kononovich, S. F. Kondakov, V. A. Merzhanov, L. I. Chernyshova, and I. F. Shchegolev, *Pis'ma Zh. Eksp. Teor. Fiz.* **46**, 211 (1987) [*JETP Lett. Suppl.* **46**, S181 (1987)].
- ²⁷M. Oda, T. Ohguro, H. Matsuki, N. Yamada, and M. Ido, *Phys. Rev. B* **41**, 2605 (1990).
- ²⁸R. Yoshizaki, N. Ishikawa, H. Sawada, E. Kita, and A. Tasaki, *Physica C* **166**, 417 (1990).
- ²⁹G. Shirane, Y. Endoh, R. J. Birgeneau, M. A. Kastner, Y. Hidaka, M. Oda, M. Suzuki, and T. Murakami, *Phys. Rev. Lett.* **59**, 1613 (1987).
- ³⁰K. B. Lyons, P. A. Fleury, J. P. Remeika, A. S. Cooper, and T. J. Negran, *Phys. Rev. B* **37**, 2353 (1988).
- ³¹K. B. Lyons, P. A. Fleury, L. F. Schneemeyer, and J. V. Waszczak, *Phys. Rev. Lett.* **60**, 732 (1988).
- ³²H. Takagi, T. Ido, S. Ishibashi, M. Uota, S. Uchida, and Y. Tokura, *Phys. Rev. B* **40**, 2254 (1989).
- ³³A. Kampf and J. R. Schrieffer, *Phys. Rev. B* **41**, 6399 (1990).